UDC 621.314 https://doi.org/10.20998/2074-272X.2026.2.10

N.T. Vinh, D.T. Anh

Bidirectional DC/AC converter for flexible distributed energy integration into AC microgrids

Introduction. *This work focuses on the development of microgrids in remote areas, islands and regions frequently affected by natural disasters, particularly in Vietnam and other island countries in Asia.* ***Problem.*** *The converters perform direct and isolated energy conversion to AC or DC microgrids, which are distributed grids that integrate various distributed energy sources, including renewable energy such as wind power, solar power and others. To enable the system to operate continuously providing stable power, improving the efficiency and effectiveness of distributed power sources by providing a suitable circuit design to limit losses on the main switches and the number of switches and passive components in the converter is minimal. The* ***goal*** *is to develop the internal structure of a boost DC converter into a multi-port converter connected to the storage system and the AC microgrid under the condition of reducing the main switching losses with the condition of intermittent charging of the storage system during the operating period of the solar power source.* ***Methodology.*** *The study uses the switching adjustment method and modeling simulated to analyze the operating conditions adapted to the application system.* ***Results.*** *Analytical expressions were derived for calculating currents, voltages, losses on components, main switches, and conventional switches. The influence of storage circuit switching on reducing losses in the main switch is shown for the operating cases.* ***Scientific novelty.*** *Using the developed simulation model, new expressions were derived that allow us to establish operational dependencies that reveal the relationships between the parameters of the storage device's switching components. These dependencies determine the efficiency and performance of the operational function, meeting the requirements of the microgrid system.* ***Practical value.*** *Enhance the efficiency of utilizing distributed energy sources and improve the conversion efficiency of flexible operation converters for AC or DC microgrids in the power system.* References 30, tables 2, figures 22.
Key words: **boost DC/DC converter, battery, DC/DC full bridge, bidirectional DC/DC and DC/AC converters.**

Вступ. *Робота присвячена розробці мікромереж у віддалених районах, на островах і в регіонах, часто схильних до стихійних лих, зокрема у В'єтнамі та інших острівних країнах Азії.* ***Проблема***. *Перетворювачі здійснюють пряме та ізольоване перетворення енергії в АС або DC мікромережі, які є розподіленими мережами, що інтегрують різні розподілені джерела енергії, включаючи відновлювані джерела, такі як вітрова, сонячна енергія тощо. Для забезпечення безперервної роботи системи та стабільного електропостачання необхідно підвищити ефективність розподілених джерел енергії за рахунок відповідної схемотехніки, що обмежує втрати на головних перемикачах, а також мінімізувати кількість перемикачів та пасивних компонентів у перетворювачі.* ***Мета*** *полягає в розробці внутрішньої структури підвищувального DC перетворювача в багатопортовий перетворювач, підключений до системи накопичення енергії і АС мікромережі, за умови зниження втрат на головних перемикачах і періодичної зарядки системи накопичення енергії протягом періоду роботи сонячного джерела енергії.* ***Методика***. *У роботі використовується метод регулювання перемикання та моделювання для аналізу умов експлуатації, адаптованих до системи застосування.* ***Результати***. *Отримані аналітичні вирази для розрахунку струмів, напруг, втрат на компонентах, головних та звичайних перемикачах. Для різних режимів роботи показано вплив перемикання кіл накопичувача на зниження втрат у головному вимикачі.* ***Наукова новизна***. *За допомогою розробленої імітаційної моделі отримано нові вирази, що дозволяють встановити операційні залежності, які розкривають взаємозв'язки між параметрами комутаційних компонентів накопичувача. Ці залежності визначають ефективність та продуктивність операційного режиму, що відповідає вимогам мікромережевої системи.* ***Практична значимість***. *Підвищення ефективності використання розподілених джерел енергії та покращення коефіцієнта перетворення гнучких перетворювачів для АС або DC мікромереж в енергосистемі.* Бібл. 30, табл. 2, рис. 22.
Ключові слова: **підвищувальний DC/DC перетворювач, батарея акумуляторів, повний DC/DC міст, двонаправені DC/DC і DC/AC перетворювачі.**

Introduction. A comprehensive overview of the micro-AC grid multi-port converter topology has been presented in [1–5]. In recent years, our society has caused numerous negative environmental impacts through the intensive use of traditional energy sources. In addition, the deterioration of the distribution system and the increasing demand for electrical energy has made this concern evident. Although there have been many promising developments in energy decentralization using renewable energy sources in recent years [6]. The increasing penetration of renewable energy sources into the conventional AC grid may cause other problems such as voltage and frequency instability [7].

To address these issues, concepts such as microgrids, minigrids and smart grids for future distribution systems have been researched and put into practice. The microgrid concept was initially proposed in [8]. Its operating principle involves aggregating multiple micropower sources and loads into a system-like model that includes these components and enables either stand-alone or grid-connected operation [9]. Therefore, to optimize the grid appropriately using both AC and DC hybrid systems in the ongoing and future smart grid, typical hybrid microgrid architecture is proposed to reduce the number of power converters in standalone AC or DC systems and to promote the interconnection of different AC and DC sources and loads as a multi-energy system. In this architecture, power routers aim to minimize losses in power distribution [10], energy management for hybrid microgrids using conventional transformers is an inflexible constraint for operations [11–13]. In contrast to AC or DC power grids, the control, system management and operation of hybrid microgrids are more complex. This structure can provide the following contents:

1) Hybrid microgrids can flexibly supply power loads from both DC and AC subgrids, thus system reliability can be improved by feasible alternative power sources [14].

2) Each DC source can be easily connected to the DC line by simply adjusting the DC voltage to limit the starting current.

3) System costs and losses are reduced because some power conversion stages are eliminated for both DC source and load components.

4) The system can be expanded more easily because DC converters can be installed in parallel.

In hybrid renewable energy systems, components such as unidirectional AC/DC converters are used to connect sources to the grid, sources to stored energy, or to perform a single operating function in one direction only. Bidirectional converters handle one load and are capable of connecting two AC and DC grids. DC/DC converters

© N.T. Vinh, D.T. Anh

are employed for DC grids, and multi-output DC/DC converters serve different loads [15–18], the literature has some limitations in the existing multi-port converter topologies, and further research is needed in this area. Renewable energy-based power systems may use dual-input single-output converters [19]. The solar power system, which includes a DC/AC converter, has many components that limit the conversion efficiency [20]. Similarly, portable devices also utilize dual-input single-output converters [21]. For low input voltages corresponding to renewable energy sources there is a family of three-switched multi-input DC/DC converters [22]. The DC/DC converter can work with low voltage sources [23]. Dual-port, multi-output DC/DC converter converts energy in one direction [24, 25]. Later, many other topologies were derived from this basic series of converters [26, 27]. Multi-input and multi-output converters [28] are often used for hybridization between renewable energy sources and electric vehicles for higher efficiency, lower cost and higher reliability. With different current, voltage characteristics are proposed in the DC/DC converter [29] has many components that destabilize the energy conversion. In this topology, the voltage stress on the switch is reduced by increasing the output voltage level.

The converter structure proposed in this work is implemented in a system with a block diagram (Fig. 1). This system can operate to meet different voltage parameter requirements and integrate several distributed power sources to handle changing loads. Sources can be used independently or simultaneously with this structure if connected in parallel with the DC line connected right inside the DC/DC phase conversion converter with simple, low-volume switching components.

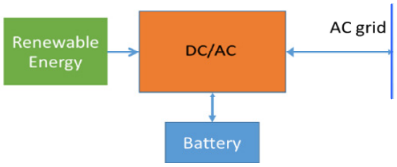

Fig. 1. Schematic diagram of a microgrid system using a DC/DC/AC converter

The advantages of the proposed topology over the topologies in the cited papers are:

- it can connect multiple input sources or a single input source at the same time;
- it can power multiple loads with different voltage levels;
- in addition to providing regulated output power to the load, this converter can harvest maximum power from input sources.

The **goal** is to develop the internal structure of a boost DC converter into a multi-port converter connected to the storage system and the AC microgrid under the condition of reducing the main switching losses with the condition of intermittent charging of the storage system during the operating period of the solar power source. The new topology assimilates multiple renewable energy sources and powers multiple loads with different output levels. Energy is converted in two directions for each stage and case, according to the requirements of the source and load.

Proposed converter operating case. The proposed converter is designed to provide an AC load output and to receive input from the AC grid and a renewable energy source, such as distributed energy, in each operating case. This converter is developed by integrating boost converters, buck-boost bidirectional converters, and H-bridges. Figure 2 shows the circuit diagram of this combination.

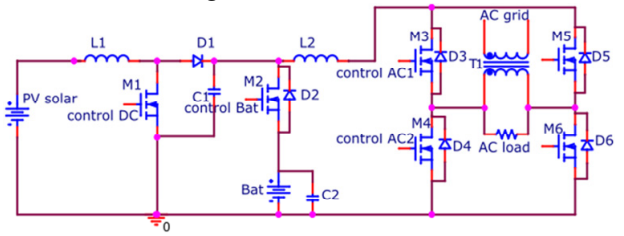

Fig. 2. Proposed DC/DC/AC converter combining power source, DC load, AC load, storage system and AC microgrid

The converter is linked by wind power or solar battery in this paper using solar power, a storage system port denoted by Bat (could be an electric vehicle-EV) and an output load port is AC grid. Two independent inductors with inductances L1 and L2 facilitate energy exchange in 2 basic boost converters, which include an electronic switch M1 connected to a PV source. In this structure, it is possible to add more energy sources to the circuit by connecting additional boost circuits in parallel to the input point of the energy storage circuit. Furthermore, L2 is connected to an H-bridge circuit to enable bidirectional operation. The converter is equipped with 6 power electronic switches: M1 and M2, as well as the switch group M3–M6. These switches can be controlled independently, and each power switch group can be adjusted based on the converter's operating conditions. The switches are the main elements that convert energy from the inverter ports: PV sources, storage systems, AC, DC loads and microgrids. M1 is responsible for efficient energy conversion from a PV power source. Diode D2 is responsible for maximum energy transfer to AC and DC loads, M2 converts energy taken from PV power source and AC grid.

To analyze the proposed converter, certain assumptions are made, as follows:

- all switches ideally conduct reverse blocking;
- all connected renewable energy sources are assumed to supply DC voltages at their maximum power points.

The following are the possible cases that can be described according to the different input and output operations of this new converter. Each case of this converter operating in a steady state will be analyzed independently in the following sections.

**Case* 1. In the first case of the converter shown in Fig. 3, energy from solar renewable sources supplies power to the storage system. Additionally, it can feed the DC load, which is sourced from VC1, as well as the loads at the AC supply grid, including the AC source and other loads. The accumulator system is charged during the conversion. The converter is implemented based on the DC/DC circuit principles of boost, buck, and H-bridge. A single-phase H-bridge is connected to the AC supply grid. The H-bridge circuit is connected to the AC grid via transformer T1, as shown in Fig. 3. The circuit connected to the storage system acts as a buffer circuit for the DC/DC converter at the key switch M1, helping to consume the leakage energy of the coil L1. The voltage to the DC/AC converter is limited by the voltage on the Bat storage system:

$$U_{C1} = U_{pv}\frac{1}{1-d_1}; \tag{1}$$

$$U_{Bat} = U_{C1}d_2, \tag{2}$$

where d_1, d_2 are the duty cycle of M1 and M2 respectively; U_{C1} is the output voltage of DC/DC converter stage.

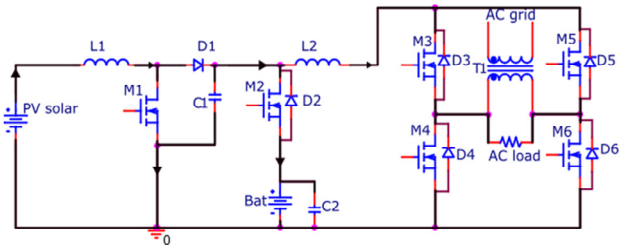

Fig. 3. Schematic diagram in case 1

This mode of operation can be applied when multiple distributed energy sources are available, and maximum power can be obtained with the addition of Boost converters. In addition to boosting the power to the load, the excess energy can be stored for later use. When the Bat is charging in this mode and M2 will control the Bat charging voltage and will close when the Bat is fully charged, or the input voltage increases to a certain value. The transfer of energy from the source to the load depends on the control strategy used to generate gate signals that control the input and output switches. This strategy is based on the availability of the input source, the load conditions, and the status of storage devices.

The voltage across the main switches M1 and M2 is:

$$U_{M1} = U_{D1} + \frac{U_{pv}}{1-d_1}; \tag{3}$$

$$U_{M2} = \frac{U_{pv}}{1-d_1} - U_{Bat}. \tag{4}$$

Current M1 is expressed as:

$$i_{M1} = \frac{(u_{pv} - u_{M1})d_1}{L1} + i_0, \tag{5}$$

where i_0 is the initial operating current of the converter.

When M2 has d_2 operating to conduct current, the current through switch M2 is:

$$i_{M2} = i_{D1} - i_{C1}. \tag{6}$$

Conduction loss power is:

$$P_{condMOSFET} = U_{DS\_M1} \cdot I_{DSM1} + r_{M1} \cdot I^2_{DS\_M1} + \ldots$$
$$\ldots + U_{DS\_M6} \cdot i_{DS\_M6} + r_{M1} \cdot I^2_{DS\_M6}, \tag{7}$$

where U_{DS} is the junction voltage when the MOSFET switch is turn-on; I_{DS} is the drain-to-source current of the MOSFET.

Power loss during switching is:

$$P_{loss\_sw} = f_{sw} \cdot (W_{on} + W_{off}), \tag{8}$$

where W_{on}, W_{off} are the energy dissipation during turn-on and turn-off times, respectively [30]; f_{sw} is the switching frequency of switches M1 and M2.

Conduction loss power of diode D1 is:

$$P_{loss\_D1} = f_{sw} \cdot V_{D1} \cdot I_{D1}, \tag{9}$$

where V_{D1}, I_{D1} are the voltage, current of D1 during the time for current to pass.

Power losses of LC component in the converter are:

$$P_{L1} = R_{L1} \cdot I^2_{L1rms}; \tag{10}$$

$$P_{L2} = R_{L2} \cdot I^2_{L2rms}; \tag{11}$$

$$P_{C1} = R_{C1} \cdot I^2_{C1rms}, \tag{12}$$

where R_{L1}, R_{L2}, R_{C1} are the internal resistances of coils L1, L2, C1; I^2_{L1rms}, I^2_{L2rms}, I^2_{C1rms} are the effective currents through coils L1, L2, C1.

Total power loss in the converter in case 1 is:

$$P_{loss\_case1} = P_{condMOSFET} + P_{loss\_sw} + \\ + P_{loss\_D1} + P_{L1} + P_{L2} + P_{C1}. \tag{13}$$

In which d_1 and d_2 are the opening times of M1 and M2, respectively, and they have different values to ensure that the output voltage of bridge H is stable. As a result, the opening time of M2 (d_2) is delayed compared to that of M1 (d_1). As expression (1) we see an advantage of this circuit is that the opening time of the locks is always less than 1/2 of the working cycle of the converter.

Bat is charged with current when the switch M2 is active and if the PV source voltage is less than Bat voltage then the PV supply diagram is considered to be inactive. This is also a value to set the working threshold for the PV source to supply to the load.

**Case* 2. Figure 4 shows the schematic diagram for case 2. The required AC and DC load power is supplied so that the storage system will temporarily suspend the charging state. The charging circuit of lock M2 does not operate. Due to many reasons such as the energy from the PV source not being enough to meet the load (cloudy weather), the AC and DC load increasing, or the storage system is fully charged. The converter operates according to the DC/DC boost circuit principle combined with the H-bridge. The switches M1 and M3–M6 work on the DC/DC boost converter and the DC/AC H-bridge circuit (converting energy to the AC grid).

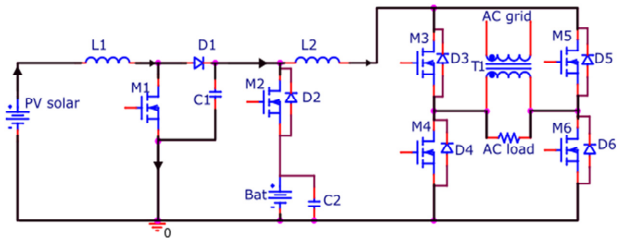

Fig. 4. Schematic diagram in case 2

**Case* 3. In case 3 (Fig. 5) AC and DC loads are supplied from PV power source and storage system. In this case, PV power source reduces capacity, the load increases, and the AC grid is at a high load time, so the storage system generates additional energy to supply the load. At this time, the circuit has M1 active, D2 active, and M3–M6 active.

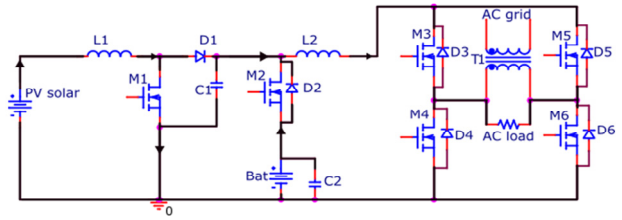

Fig. 5. Schematic diagram in case 3

**Case* 4. Case 4 operations (Fig. 6) the Bat storage source energy supplies the load and the AC grid, the switch M1 is not working, the PV energy source is not working because of the weather at night. M2 is not working, and the energy is transmitted through D2 and L2 to the H-bridge circuit. In this case, the microgrid load is used under priority conditions because of the limited energy source from the storage system.

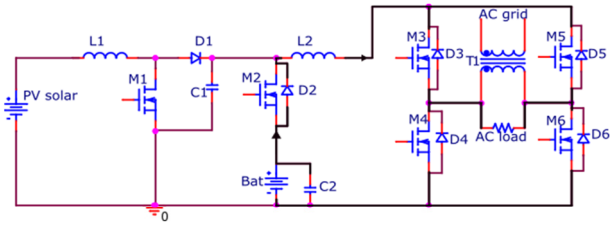

Fig. 6. Schematic diagram in case 4

**Case 5*. Case 5 operations (Fig. 7) excess solar energy is supplied to the DC load. Meanwhile, the AC load receives sufficient and surplus energy from the AC grid. As a result, the energy from PV sources and the AC grid becomes redundant, leading to the accumulation system being charged from both sources. This case arises when distributed energy sources are built locally close to each other in an area. The circuit operates in this case as follows: M1, M2 and M3–M6 operate according to the Boost principle and H-bridge circuit.

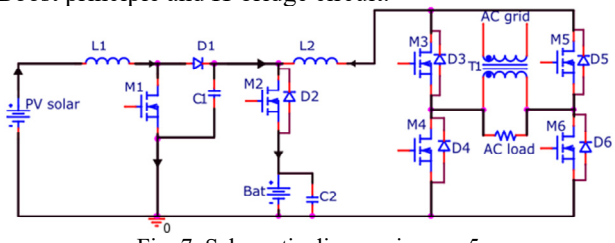

Fig. 7. Schematic diagram in case 5

**Case* 6. This case of the converter system assumes that the AC grid power source is sufficient and has surplus power to supply the AC load, leading to the converter operating independently of the AC grid. The PV power source supplies Bat storage and the DC load if any. The converter operates as a DC/DC boost in which M1 and M2 are active, and the H-bridge circuit is inactive. The PV power is always used thoroughly and efficiently. The operation of case 6 is depicted in Fig. 8.

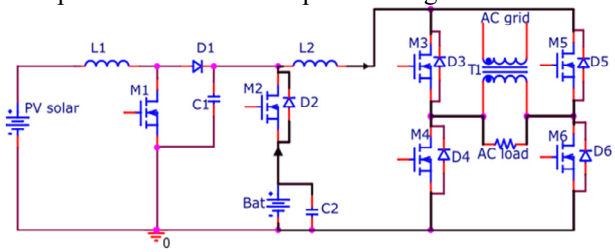

Fig. 8. Schematic diagram in case 6

**Case* 7. Figure 9 describes this case of the converter assuming that renewable energy sources stop producing energy (wind sources need to stop operating or maintenance due to natural disasters or weather, solar energy sources at night). In addition, the load-side energy source connected to the AC grid system is connected to another source of energy with excess energy; then the energy is converted from the AC grid to the DC load and the Bat storage system through M3–M6 and M2 locks in operation.

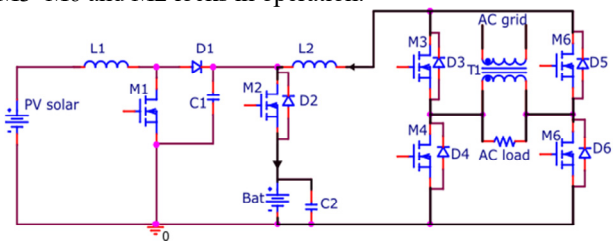

Fig. 9. Schematic diagram in case 7

In the seven working cases, case 1, case 3 and case 5, the main switches M1, M2, and the common switch H-bridge in the proposed converter perform full operation. These cases all demonstrate the loss limitation process for the main switch M1 when there is a storage connection circuit. The stress voltage on switch M1 is limited to a maximum of the rated voltage on the battery. The regulating switches in the converter play a crucial role in managing operations for real-world scenarios. They account for the requirements of each load and the capacity of the regulating sources, ensuring the optimal use of renewable energy from the AC microgrid and PV distributed sources connected to the storage system. The flexible DC/DC/AC converter proposed has the following highlights:

1. There are 7 cases to convert energy to optimize electric energy from renewable energy sources, storage systems, and energy sources from the grid. Flexibly adjust sources and loads according to the priority conditions of the load (electricity customers). Increase the stability of the continuous power supply for the load (when there is a power outage due to incidents or natural disasters). For converters [1–5], which only perform certain functions for identifying the maximum point of the distributed energy source supplied to the load, the load depends on the capacity of the source or storage system. Additionally, the system does not utilize coordination from energy sources in the AC microgrid.

2. In the principal circuit, multiple sources can be connected by placing the connection structures in parallel with the connection point of capacitor C1 (Fig. 2). This method allows for many distributed input sources to pass through the proposed converter without altering its internal structure. However, this approach may complicate the control system. In contrast, converters described in [26, 27] are limited to only one or two input sources.

3. The converter limits the stress voltage on the switch M1 when adjusting the charging mode for the appropriate storage system when the right time the switch M1 changes state from open to closed, the switch M2 opens for a period of time shorter than the closing time of the switch M1 to dissipate the leakage energy of the coil L1.

Control engineering. In this converter, there are 6 electronic switches to control with the cases analyzed in the above section described as Fig. 10 using the PWM technique for main switches M1, M2 and SPWM for the H-bridge.

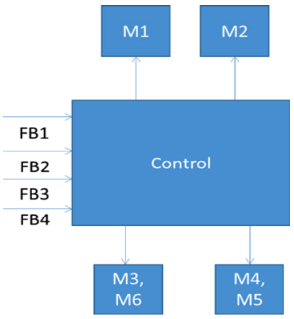

Fig. 10. Control block diagram for mixed-source DC/DC/AC converter

Each case of control mode will be implemented differently with the goal that the output voltage connected to the H-bridge circuit of the converter is almost stable and finds the largest power points from renewable energy sources and storage systems. Therefore, the control circuit has current and voltage feedback loops and uses the

maximum power point finding method for the converter. From specific terminals such as current and voltage on Bat; current and voltage on AC and DC loads; current and voltage on PV source and AC grid to determine the energy status of the terminals connected to the converter. From those parameters to give control commands according to the operating cases of the converter in accordance with the goal of optimal use of energy from the PV source.

**Case 1 – PV supplies energy to Bat, AC, DC loads, and AC grid.* The control mode for this case has the following basic components and requirements for the control circuit:

1) Implement the algorithm to find the maximum power point for the 2 mixed energy sources;

2) Adjust the output voltage to stabilize the load or connect to the AC grid and DC grid;

3) Implement the charging mode control for Bat. Switches M1 and M2 perform control using a PWM control technique along with controlling switches M3–M6 according to the feedback signal from the storage system and the AC microgrid output current and voltage to perform appropriate control.

**Case 2 – PV supplies energy to AC grid, DC and AC loads.* In the converter, the energy feedback signal on the Bat is full or needs to supply power to the AC or DC load, leading to the control circuit for the charging circuit for the Bat not working and stopping charging from the renewable energy source and only supplying power to the AC grid through the H-bridge DC/AC converter. Pulse width modulation for the switch M1 is calculated as the formula in the basic boost converter so that the voltage to the H-circuit is stable.

**Case 3 – PV and Bat supply power to AC, DC loads, and AC grid.* This mode is intended for the power source to the AC grid and DC load to be supplied from PV and Bat solar power. The feedback signal from the feedback loops confirms to modulate the pulse width for the electronic switch M1, M3–M6 is calculated as the formula in the basic boost converter and H-bridge.

**Case 4 – Bat supplies power to AC grid.* This mode is intended for the power source to the AC grid to be supported from the Bat source when it is dark, and the PV renewable source is no longer generating electricity. There is essentially an independent DC/AC conversion circuit from Bat to the AC load. The feedback signal is confirmed to be sent back to control the M3–M6 switches to operate as a DC/AC circuit.

**Case 5 – PV energy and AC grid supply the AC and DC storage and load systems together*. At this time, PV energy generates well (DC load decreases), AC grid has excess energy (AC load decreases). There are essentially 2 DC/DC and AC/DC conversion circuits. Feedback signals from the feedback loops make control decisions for the M1, M2, and M3–M6 switches according to the corresponding principle as the circuit above.

**Case 6 – PV source supplies energy to Bat.* Converter works independently of the AC grid, the AC load demand is fully supplied from the AC grid. Besides, the PV source is still generating electricity, the Bat is not fully charged yet. The control signal will command M1 and M2 to operate.

**Case 7 – AC grid supplies power to Bat.* This mode is intended to supply power to Bat from the AC grid when there are no renewable energy sources. This situation will arise when Bat is fully discharged or under-powered. Control signal for switches M2 and M3–M6 AC/DC H-bridge circuit.

Simulation results. The proposed converter model discussed above is simulated using Orcad software corresponding to the operating cases. The simulation model is based on the actual operating situation of the system when the converter is connected and to verify the analytical results obtained in this section. The parameters used for simulation study are predetermined and are presented in Table 1. The input voltage corresponds to the voltage level of small renewable energy sources such as solar panels, fuel cells and small wind turbines. The output voltage is designed to power low power electronic devices, and the output voltage is designed to charge a 200 V Bat storage battery. The performance of the converter under different operating conditions in open-loop and closed-loop systems is evaluated and discussed in this section.

Table 1

System parameters for simulation studies

Parameter	Value
PV source voltage, V	75–180
Battery voltage, VDC	200
AC grid, AC load	220 V, 50 Hz
DC load, V	250
Inductance L1, L2, μH	10
Load capacitance, μF	10
Electronic switch	MOSFET
DC/DC switching frequency, kHz	50
DC/AC switching frequency, kHz	30

Simulation for case 1. The simulation model for the converter is shown in Fig. 2. In this model, the input source varies with the environmental changes, so in addition to supplying power to the load, additional power is stored.

The proposed inverter operating mode involves 3 components, i.e., PV source, Bat and AC, DC load. This mode will operate during the day when PV source is good. The aim of this mode is to utilize maximum power from PV and can connect a wind source to supply power to AC load and storage. This objective needs to be achieved while ensuring maximum power point tracking of PV source.

Figure 11,*a* shows the reverse breakdown voltage value of 240 V for the M1 and M2 switches at the V(M1:2) probe, from which we can get the parameter value to select the appropriate electronic switch for the circuit. In the M1 voltage graph, an image of the parasitic parameter of the MOSFET is seen during the off period, this effect increases the actual loss of the MOSFET. The output voltage of the load is close to 250–400 VDC at the V(L2) probe. Current through the components L1, M1, M2 in Fig. 11,*a*, the current values through the inductance components L1 at the PV power source.

Figure 11,*b* shows the total power values at the sources and the loads in the whole system. We can see the sources at the loads, including the 2nd and 3rd measuring terminals. From the values, we can simply calculate the efficiency of the conversion system in this case when changing the input power value.

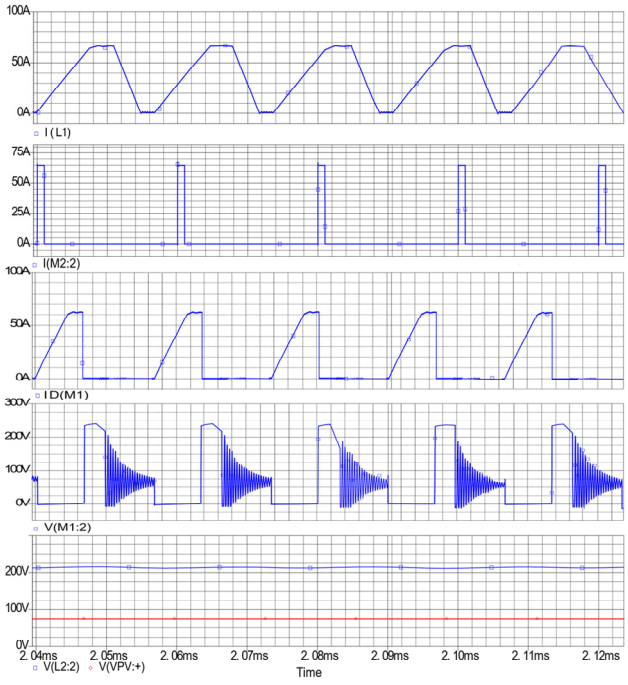

a

b

Fig. 11. Graph during case 1 operation:
a – current and voltage diagrams of the elements in the circuit;
b – active power of PV input and AC load

Simulation for case 2. This case involves 2 components – PV source and AC load. From Fig. 12,*a* it is observed that the reverse voltage on M1 is the same as in case 1, but the load decreases due to no power supply to Bat, so it is necessary to adjust the control pulse width for M1 to decrease. Figure 12,*a* results of measuring the current value through the load and through the M1, L1 switches compared to scenario 1. Figure 12,*b* shows the power value of two PV source components and AC load. The energy part at the load value is determined by the PV input voltage parameter of 75 V.

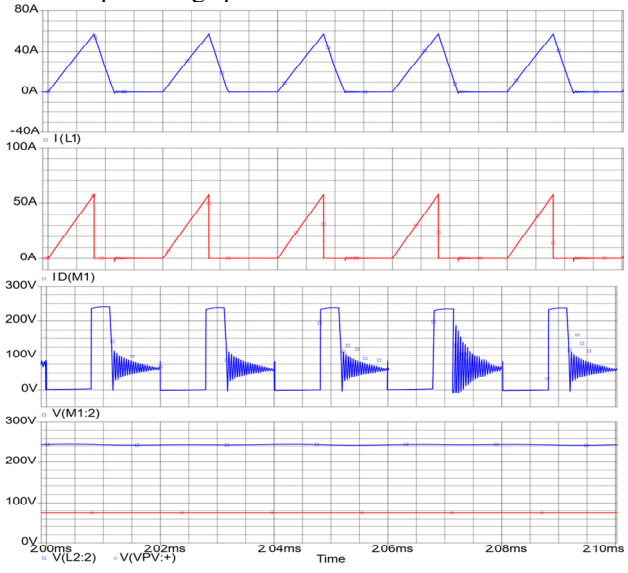

a

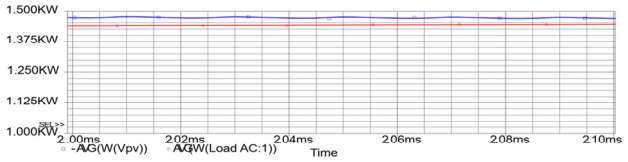

b

Fig. 12. *a* – current and voltage diagrams of the elements in the circuit; *b* – active power of PV input and AC load in case 2

Simulation for case 3. This mode is active when the battery is fully charged as well as when the PV still gets enough light to produce electricity. The purpose is to supplement the energy from storage to the load at AC and DC. From Fig. 13,*a* we have the simulation diagram of the conversion system in this case, this implies that the control for this mode is active, and it is verified.

Figure 13,*b* shows the power measurement results of 3 components in the power supply circuit of the Bat power supply.

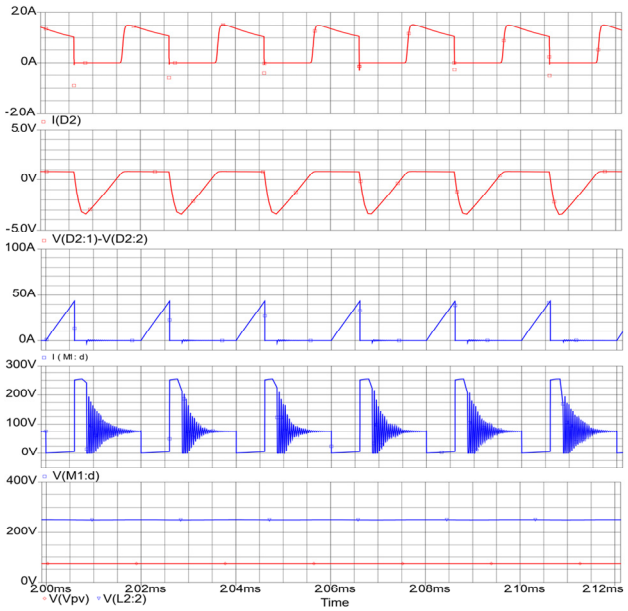

a

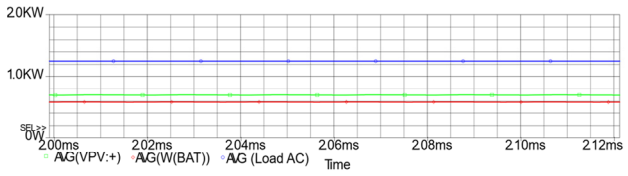

b

Fig. 13. *a* – simulation diagram of case 3; *b* – power on 3 ports

Simulation for case 4. Similarly, in this case, Fig. 14 illustrates the measurement results of the battery storage power supplied to the AC load, as well as the current and voltage patterns of the circuit elements during the energy conversion process. With this energy source, it is possible to provide partial stabilization for the entire system when there is a shortage of energy in the AC microgrid.

Simulation for case 5. The power measurement results of the storage and AC load supplied by PV energy source and AC grid are shown in Fig. 15. With this energy source it can provide partial stabilization for the storage system as well as the load side that is reducing the power flow.

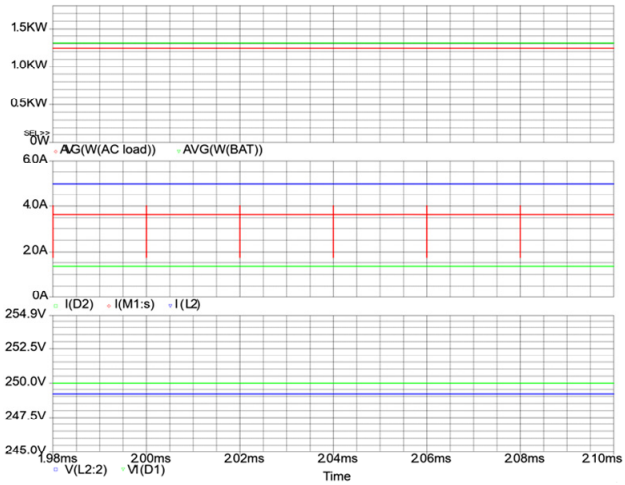

Fig. 14. Simulation activity graph of case 4

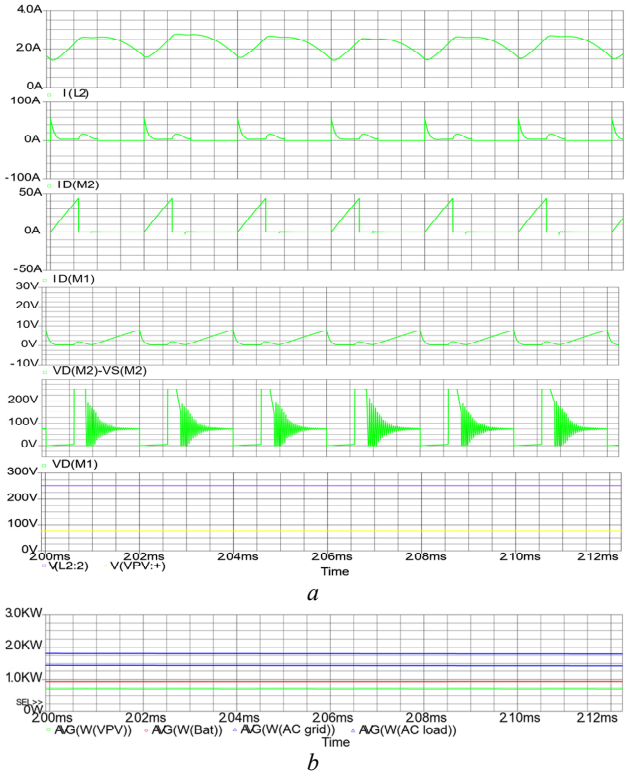

a

b

Fig. 15. Single-input (*a*), dual-output (*b*) power graph in case 5

Simulation for case 6. Figure 16,*a* shows the voltage and current values on the elements M1, M2, and L1, the input voltage for the storage system. Figure 16,*b* shows the input and output power values to determine the efficiency of this conversion process.

Simulation for case 7. In 7 case H-bridge circuits are working, the current and voltage signals on elements M2 and L2 are shown in Fig. 17,*a*. Figure 17,*b* shows the power values of the AC load, AC grid and Bat.

Figure 18 shows the simulation results of the performance of the DC/DC/AC converter with different power values for each specific case, the maximum working power is 2500 W, PV voltage is 75 V. The voltage change of the power supply input is shown in some cases with PV power supply.

When the load demand energy changes at the AC microgrid, it affects the energy conversion process from the energy source supplied from PV with each mode of increasing or decreasing the energy consumption, the change time is 5–10 ms to reach the change value when decreasing as shown in Fig. 18. The fluctuation amplitude is about 10 % compared to the new change value.

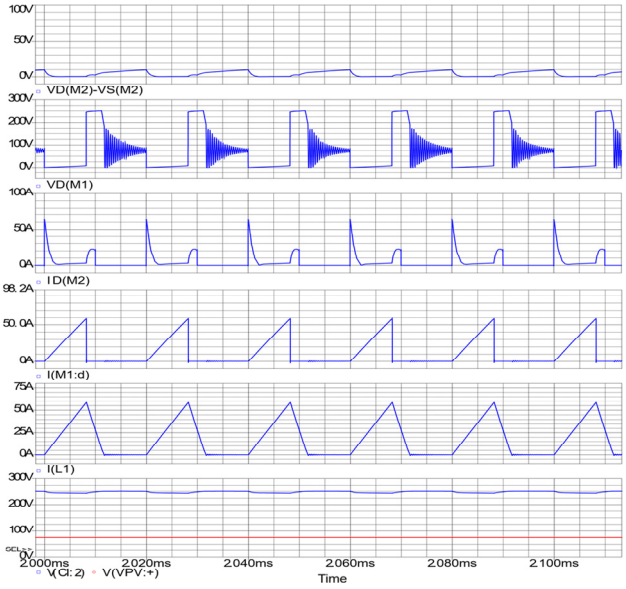

a

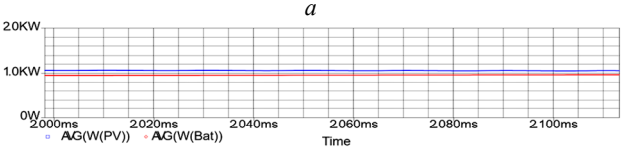

b

Fig. 16. *a* – voltage-consistent signal; *b* – input and output power values

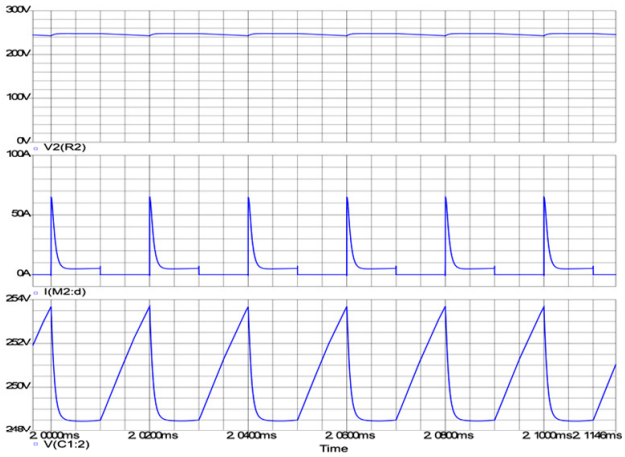

a

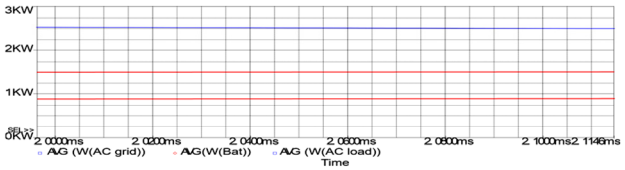

b

Fig. 17. *a* – simulated current, voltage; *b* – gate power in case 7

Figure 19,*a* cases 1, 2, 3, 5, 6 show the power efficiency for the specific cases, where the higher efficiency value is in cases 2 and 3 near 96.9 % at 500 W operating power. The low efficiency value is near 94.2 % at 2500 W operating power in case 6 in the converter. Figure 19,*b* depicts the overall efficiency of the converter for the 7 cases.

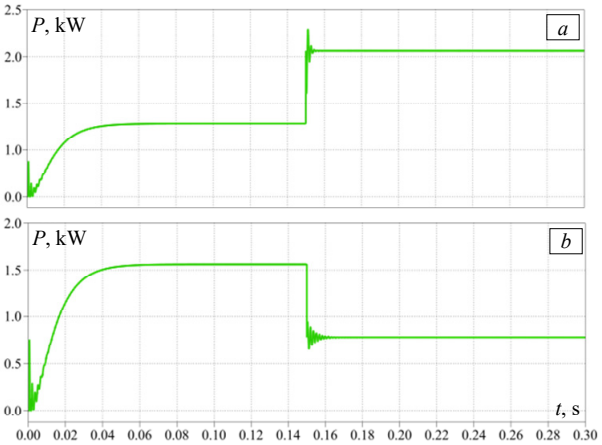

Fig. 18. AC load at $t = 0.15$ s for case 1:
a – AC load increase 610 W; *b* – AC load decrease 750 W

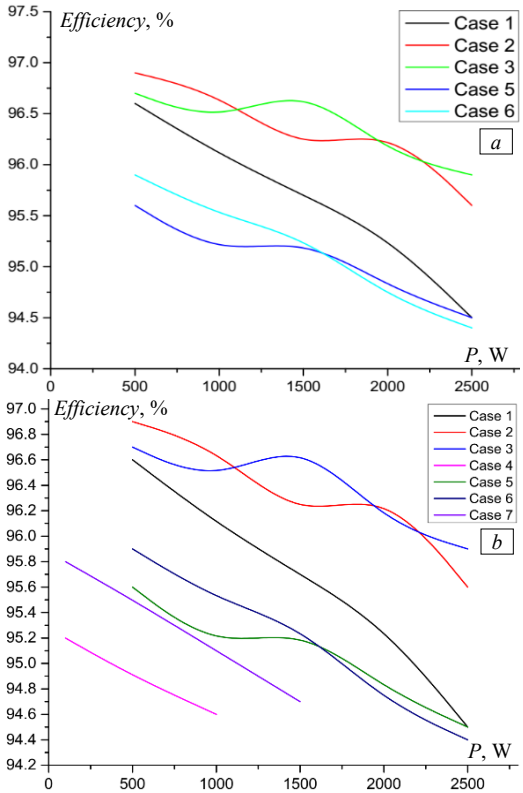

Fig. 19. Simulation results of the performance of the converter operation cases (*a*) related to the operation of PV sources (5 cases); *b* – all cases (7 cases)

Experimental results. Figure 20 shows the experimental DC/DC/AC converter at the following parameters: input voltage value 75–180 VDC; AC load capacity 500–2500 W.

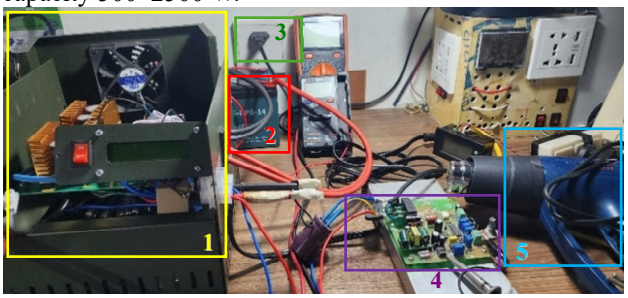

Fig. 20. Experimental image of flexible converter:
1 – converter; 2 – storage; 3 – single-phase AC grid;
4 – DC source; 5 – single-phase AC load

Table 2 shows the input and output parameters of the converter at the ports.

Table 2

Experimental parameters

DC/DC boost input voltage, VDC	75–180
DC/DC boost output voltage, VDC	250
Inductances L1, L2, μH	10
Bat capacitor, μF	10
Boost circuit output capacitor, μF	10
Diodes D1, D2	Mur1560
MOSFET switch M1	IRF740
MOSFET switch M2	IRFP640N
MOSFET switches M3–M6	IRF340
DC load, Ω	500
AC output voltage, V	220±3 %
AC input voltage, VDC	200–350
AC load frequency, Hz	50±0.5 %

Figure 21 shows the experimental operation modes with the largest power value change of 2500 W, the input voltage from the PV source is 75–180 V, voltage on the DC bus is 398–399 VDC can be connected to DC microgrid, the values are displayed on the voltage and power meters.

Figure 21 shows the output voltage waveform of the load under varying load conditions. The actual output voltage is a sinusoidal waveform with a frequency of 50 Hz, in harmony with the AC grid, as shown in Fig. 21,*a*.

Figure 21,*b* – the voltage from the PV source is 75 V working with the AC load capacity of more than 1000 W and the DC voltage at DC load 399 VDC.

Figure 21,*c* – the voltage from the PV source is more than 110 V working with the AC load capacity of more than 1500 W.

Figure 21,*d* – the voltage from the PV source is 75 V working with the AC load capacity of more than 2000 W.

Figure 21,*e* – the voltage from the PV source is more than 180 V working with the AC load capacity of more than 2000 W.

Figure 21,*f* – the voltage from the PV source is 110 V working with the AC load capacity of more than 2500 W.

Experimental results are given for some typical cases in the 7 operating cases of the converter. The simulated and calculated efficiency is determined at different power values with the maximum value of 2500 W (Fig. 19). It has been studied in different load capacities and operating modes with different functions of the proposed converter. The average efficiency when powered by PV power source is close to 96.2 % corresponding to power 500 W, the efficiency at 2500 W power is close to 94.5 % (Fig. 22). The average efficiency when powered from the system storage (cases 2 and 4) is 96 %. For example, there is only one mode, such as DC/DC (case 6 is 95.8 %) and DC/AC (efficiency above 95 % [15, 16]). According to the experimental results, the average efficiency of the designed converter in working with different modes is close to 95.3 % with a maximum power of 2500 W.

Figure 22 shows the experimental and simulated average performance of the converter with a difference of almost 1 % in value. This difference is basically consistent with the actual performance during the experiment because the loss values of the components in the device, the quality of the electronic components, and the quality of the printed circuit board will be larger in the

simulation. The experimental performance of the proposed converter is larger than that of the references [15, 16] with a load operating mode of less than 2500 W.

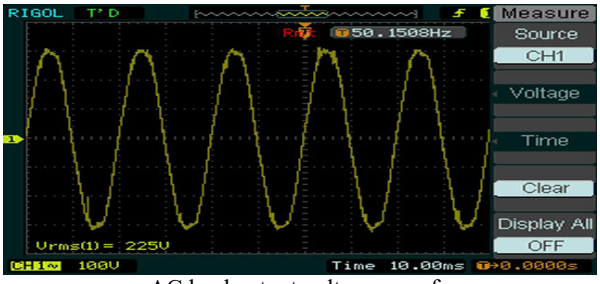

a – AC load output voltage waveforms

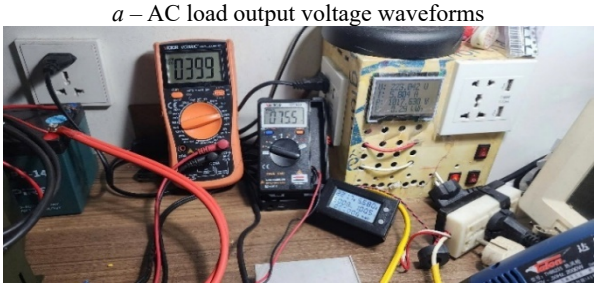

b – AC load near 1000 W

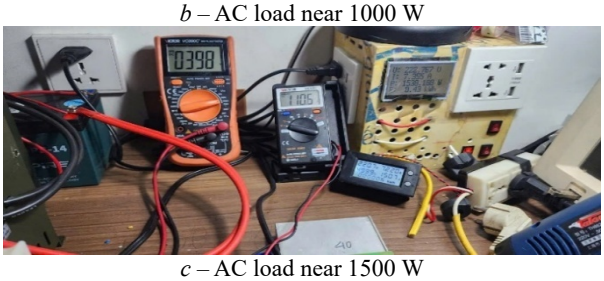

c – AC load near 1500 W

d – AC load near 1500 W

e – AC load near 2000 W

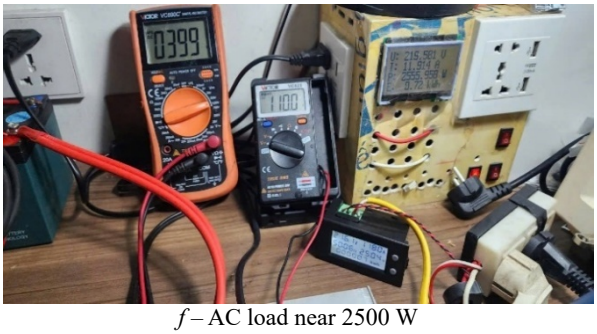

f – AC load near 2500 W

Fig. 21. AC load power values change

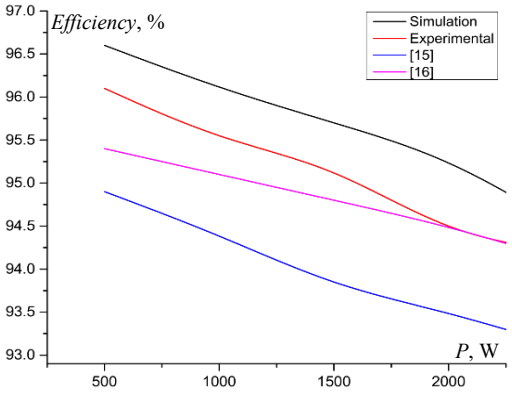

Fig. 22. Converter performance compared with references

Conclusions. The article is devoted to a multifunctional DC/AC bidirectional converter with three different independent ports, flexible operation with 7 cases, application for AC microgrids and distributed energy sources. The operating case results demonstrate 94.5 % efficiency of the converter when implemented in the system. The power circuit design creates a snubber at the storage system to limit the stress voltage on the main switch connected to the renewable energy source.

This study shows that the snubber parameters used for charging the energy storage system with recovery affect the performance, cost and design of DC/DC/AC converters in power generation and energy conversion systems.

The experimental converter basically corresponds to the simulation design and is capable of operating flexibly for systems with microgrids that can be connected to the distribution grid or work independently.

The presented research has shown the possibility of developing high-frequency non-isolated DC/DC/AC converters with low-cost performance and shows a feasible method to study new systems in the non-isolated DC/DC/AC converter family.

This solution converter increases the stability of the current grid in the Vietnamese power system. Improves the efficiency of using renewable energy sources (or distributed energy sources) contributes to national energy security.

Acknowledgments. The research team would like to thank the Science and technology project code 08-2025-HV-KTDT1 of the Posts and Telecommunications Institute of Technology Hanoi, Vietnam.

Conflict of interest. The authors declare that they have no conflicts of interest.

REFERENCES

1. Sindhuja R., Padma S. Bipolar DC output fed grounded DC-AC converter for photovoltaic application. *Electrical Engineering & Electromechanics*, 2023, no. 2, pp. 57-62. doi: https://doi.org/10.20998/2074-272X.2023.2.09.

2. Khan S.A., Islam M.R., Guo Y., Zhu J. A New Isolated Multi-Port Converter With Multi-Directional Power Flow Capabilities for Smart Electric Vehicle Charging Stations. *IEEE Transactions on Applied Superconductivity*, 2019, vol. 29, no. 2, pp. 1-4. doi: https://doi.org/10.1109/TASC.2019.2895526.

3. Alotaibi S., Darwish A. Modular Multilevel Converters for Large-Scale Grid-Connected Photovoltaic Systems: A Review. *Energies*, 2021, vol. 14, no. 19, art. no. 6213. doi: https://doi.org/10.3390/en14196213.

4. Murugan S., Jaishankar M., Premkumar K. Hybrid DC–AC Microgrid Energy Management System Using an Artificial Gorilla Troops Optimizer Optimized Neural Network. *Energies*, 2022, vol. 15, no. 21, art. no. 8187. doi: https://doi.org/10.3390/en15218187.

5. Aryani D.R., Adi F.S., Kim J.-S., Song H. An improved model-based interlink converter control design in hybrid AC/DC microgrids. *Energy Reports*, 2022, vol. 8, pp. 520-531. doi: https://doi.org/10.1016/j.egyr.2022.10.146.
6. Østergaard P.A., Duic N., Noorollahi Y., Kalogirou S.A. Recent advances in renewable energy technology for the energy transition. *Renewable Energy*, 2021, vol. 179, pp. 877-884. doi: https://doi.org/10.1016/j.renene.2021.07.111.
7. Adajah Y.Y., Thomas S., Haruna M.S., Anaza S.O. Distributed Generation (DG): A Review. *2021 1st International Conference on Multidisciplinary Engineering and Applied Science (ICMEAS)*, 2021, pp. 1-5. doi: https://doi.org/10.1109/ICMEAS52683.2021.9692353.
8. Lasseter R.H. MicroGrids. *2002 IEEE Power Engineering Society Winter Meeting. Conference Proceedings*, 2002, vol. 1, pp. 305-308. doi: https://doi.org/10.1109/PESW.2002.985003.
9. Uddin M., Mo H., Dong D., Elsawah S., Zhu J., Guerrero J.M. Microgrids: A review, outstanding issues and future trends. *Energy Strategy Reviews*, 2023, vol. 49, art. no. 101127. doi: https://doi.org/10.1016/j.esr.2023.101127.
10. Zhang D., Zhang Z., Ren Q., Tang Y., Chen X., Li Z. Research on application mode of HYBRID microgrid AC-DC microgrid in large industrial enterprise Park based on energy Router. *2022 China International Conference on Electricity Distribution (CICED)*, 2022, pp. 1715-1721. doi: https://doi.org/10.1109/CICED56215.2022.9929073.
11. Qu Z., Shi Z., Wang Y., Abu-Siada A., Chong Z., Dong H. Energy Management Strategy of AC/DC Hybrid Microgrid Based on Solid-State Transformer. *IEEE Access*, 2022, vol. 10, pp. 20633-20642. doi: https://doi.org/10.1109/ACCESS.2022.3149522.
12. Sarwar S., Kirli D., Merlin M.M.C., Kiprakis A.E. Major Challenges towards Energy Management and Power Sharing in a Hybrid AC/DC Microgrid: A Review. *Energies*, 2022, vol. 15, no. 23, art. no. 8851. doi: https://doi.org/10.3390/en15238851.
13. Li Z., Xie X., Cheng Z., Zhi C., Si J. A novel two-stage energy management of hybrid AC/DC microgrid considering frequency security constraints. *International Journal of Electrical Power & Energy Systems*, 2023, vol. 146, art. no. 108768. doi: https://doi.org/10.1016/j.ijepes.2022.108768.
14. Ayat Y., Badoud A.E., Mekhilef S., Gassab S. Energy management based on a fuzzy controller of a photovoltaic/fuel cell/Li-ion battery/supercapacitor for unpredictable, fluctuating, high-dynamic three-phase AC load. *Electrical Engineering & Electromechanics*, 2023, no. 3, pp. 66-75. doi: https://doi.org/10.20998/2074-272X.2023.3.10.
15. Suriyan K., Vennila C., Sentamilselvi M., Adhikary P., Karpoora S.K., Madhu M.C., Madhusudhana C.S., Badari N.K. A novel reconfigurable hybrid DC-AC home technique with renewable energy resources and converters. *International Journal of Sustainable Engineering*, 2023, vol. 16, no. 1, pp. 285-301. doi: https://doi.org/10.1080/19397038.2023.2205872.
16. Dharmasena S., Olowu T.O., Sarwat A.I. Bidirectional AC/DC Converter Topologies: A Review. *2019 SoutheastCon*, 2019, pp. 1-5. doi: https://doi.org/10.1109/SoutheastCon42311.2019.9020287.
17. Saafan A.A., Khadkikar V., El Moursi M.S., Zeineldin H.H. A New Multiport DC-DC Converter for DC Microgrid Applications. *2021 IEEE Industry Applications Society Annual Meeting (IAS)*, 2021, pp. 1-7. doi: https://doi.org/10.1109/IAS48185.2021.9677403.
18. Litrán S.P., Durán E., Semião J., Díaz-Martín C. Multiple-Output DC–DC Converters: Applications and Solutions. *Electronics*, 2022, vol. 11, no. 8, art. no. 1258. doi: https://doi.org/10.3390/electronics11081258.
19. Danyali S., Moradkhani A., Abdulhussein A.O., Shirkhani M., Dadvand Z. A novel multi-input medium-gain DC-DC boost converter with soft-switching performance. *International Journal of Electrical Power & Energy Systems*, 2024, vol. 155, art. no. 109629. doi: https://doi.org/10.1016/j.ijepes.2023.109629.
20. Vinh N.T. Bidirectional converter connecting the energy storage system to the DC and AC grid. *International Energy Journal*, 2023, vol. 23, no. 3, p. 141-154.
21. Vinh V.T., Vinh N.T., Dai L.V. Partly-Isolated DC-DC Converter for DC Bus Battery-PV Solar Energy System. *GMSARN International Journal*, 2022, vol. 16, no. 3, pp. 267-272.
22. Sabhi K., Talea M., Bahri H., Dani S. Integrating dual active bridge DC-DC converters: a novel energy management approach for hybrid renewable energy systems. *Electrical Engineering & Electromechanics*, 2025, no. 2, pp. 39-47. doi: https://doi.org/10.20998/2074-272X.2025.2.06.
23. Benazza B., Bendaoud A., Slimani H., Benaissa M., Flitti M., Zeghoudi A. Experimental study of electromagnetic disturbances in common and differential modes in a circuit based on two DC/DC boost static converter in parallel. *Electrical Engineering & Electromechanics*, 2023, no. 4, pp. 35-39. doi: https://doi.org/10.20998/2074-272X.2023.4.05.
24. Baazouzi K., Bensalah A.D., Drid S., Chrifi-Alaoui L. Passivity voltage based control of the boost power converter used in photovoltaic system. *Electrical Engineering & Electromechanics*, 2022, no. 2, pp. 11-17. doi: https://doi.org/10.20998/2074-272X.2022.2.02.
25. Puppala S., Singh P.P., Potnuru D. Advancements in Multiple Input Multiple Output DC-DC Converters for Efficient DC Microgrid Integration: A Scientometric Analysis. *2024 International Conference on Smart Systems for Applications in Electrical Sciences (ICSSES)*, 2024, pp. 1-6. doi: https://doi.org/10.1109/ICSSES62373.2024.10561353.
26. Al-Ameedee H.A.H., Delshad M., Shalash N.A., Fani B. Soft-Switched Non-Isolated Double-Input High Step-Up Converter With Low Input Current Ripple. *IET Power Electronics*, 2025, vol. 18, no. 1, art. no. e70051. doi: https://doi.org/10.1049/pel2.70051.
27. Themozhi G., Srinivasan K., Arun Srinivas T., Prabha A. Analysis of suitable converter for the implementation of drive system in solar photovoltaic panels. *Electrical Engineering & Electromechanics*, 2024, no. 1, pp. 17-22. doi: https://doi.org/10.20998/2074-272X.2024.1.03.
28. Carrijo de Oliveira R., Tofoli F.L., Silva de Morais A. Novel Isolated Multiple-Input, Multiple-Output Multidirectional Converter for Modern Low-Voltage DC Power Distribution Architectures. *Sustainability*, 2023, vol. 15, no. 5, art. no. 4582. doi: https://doi.org/10.3390/su15054582.
29. Maalandish M., Hosseini S.H., Sabahi M., Rostami N., Khooban M. High step-up multi input–multi output DC–DC converter with high controllability for battery charger/EV applications. *IET Power Electronics*, 2023, vol. 16, no. 15, pp. 2606-2623. doi: https://doi.org/10.1049/pel2.12587.
30. Zhu B., Liu C., Guo D., Kong L., Cai G., Sun H., Shao X. AC Voltage Synthesis Using Arbitrary Two-Phase Voltages: Frequency, Phase, and Amplitude Modulation for Direct AC–AC Power Conversion. *IEEE Transactions on Power Electronics*, 2022, vol. 37, no. 10, pp. 11855-11864. doi: https://doi.org/10.1109/TPEL.2022.3176398.

Received 24.08.2025
Accepted 07.11.2025
Published 02.03.2026

N.T. Vinh[1]*, PhD,*
D.T. Anh[2]*, MSc Student,*
[1] Faculty of Electronic Engineering I,
Posts and Telecommunications Institute of Technology,
Hanoi, Vietnam,
e-mail: vinhnt@ptit.edu.vn (Corresponding Author)
[2] College of Agricultural Mechanics, Vietnam,
e-mail: tuanhbx@cam.edu.vn

How to cite this article:
Vinh N.T., Anh D.T. Bidirectional DC/AC converter for flexible distributed energy integration into AC microgrids. *Electrical Engineering & Electromechanics*, 2026, no. 2, pp. 74-83. doi: https://doi.org/10.20998/2074-272X.2026.2.10